Modeling and Design Optimization for Pleated Membrane Filters

Yixuan Sun[1], Pejman Sanaei[2], Lou Kondic[1], Linda J. Cummings[1]

[1]Department of Mathematical Sciences, New Jersey Institute of Technology, Newark, NJ 07102-1982, USA

[2]Courant Institute of Mathematical Sciences, New York University, New York, NY 10012-1185, USA

Email: ys379@njit.edu

1. Abstract

Pleated membrane filters, which offer larger surface area to volume ratios than unpleated membrane filters, are used in a wide variety of applications. However, the performance of the pleated filter, as characterized by a flux-throughput plot, indicates that the equivalent unpleated filter provides better performance under the same pressure drop. Earlier work (Sanaei & Cummings, 2016) used a highly-simplified membrane model to investigate how the pleated membrane geometry affects this performance differential. In this work we extend this line of investigation, and use asymptotic methods to couple an outer problem for the flow within the pleated structure to an inner problem that accounts for the detailed pore structure within the membrane. By adding this level of detail, we are able to observe a decrease in particle retention by the membrane under certain conditions, which has been reported experimentally. We use our model to formulate and address questions of optimal membrane design for a given filtration application.

2. Mathematical Model

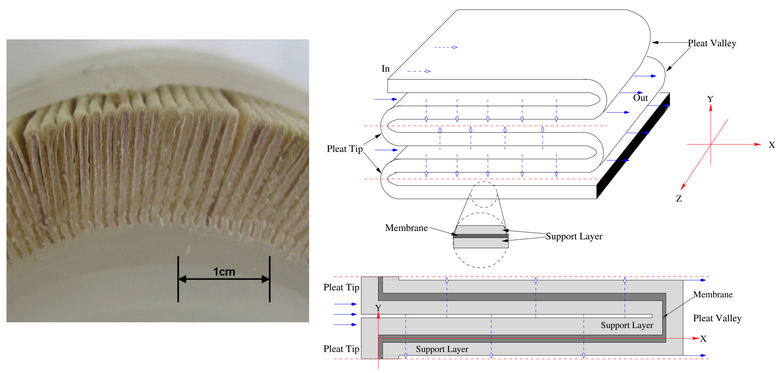

Figure 1: ***Left**: Photo of real pleated membrane (Brown 2011). **Right Upper**: Schematic, showing a few pleats. The region between the red dashed lines indicates a single complete pleat, assumed to repeat periodically. The zoom-in indicates the three-layer structure, with pale gray denoting the support layers and dark gray the membrane layer (in reality much thinner than the support layers). Blue arrows indicate the flow direction. **Right Lower**: A single pleat period, indicating how the geometry is idealized in the model, with the same color coding as the zoom-in.*

2.1 Modeling Assumptions and Governing Equations

We consider pleated filters with high pleat packing density (PPD), so that we may assume that all flow regions are occupied by either porous support material or filter membrane, with no air gaps. Figure 1 indicates how we simplify the geometry, first by neglecting dependence on the coordinate Z that runs parallel to the pleat tips/valleys; and then (if considering the cylindrical cartridge) neglecting the curvature of the cylinder. This reduces the problem to 2D in the (X,Y)-plane, where X is the direction along the pleat (from tip to valley), and Y is the coordinate perpendicular to the membrane in each pleat. We further simplify by neglecting the curvature at the pleat tip and valley, which allows us to view each pleat as one of a periodic array of rectangles. We assume each rectangle (pleat) is symmetric about the centerline ($Y = H$), which gives our simplified half-pleat domain, indicated in figure 2.

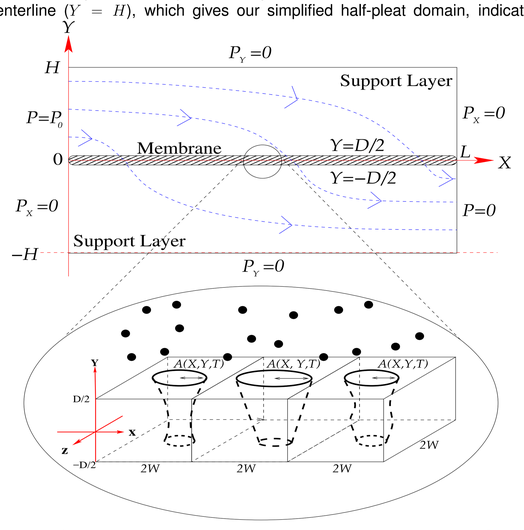

Figure 2: *Simplified domain (half the pleat) showing boundary conditions at inlet and outlet and schematic streamlines. Symmetry is assumed within each pleat at $Y = H$. Zoom-in shows the membrane pore morphology, with each pore assumed to lie within a square period-box of size 2W.*

We assume that Darcy's law governs flow in both the support layers and the filter membrane. Both are porous media, though the support material has a much higher permeability (K) than that of the membrane ($K_{\rm m}$): $K \gg K_{\rm m}$. Support permeability K is assumed to be constant in both space and time, reflecting an assumption that fouling of support layers does not occur. The velocity $\mathbf{U} = (U,V)$ within the support layers is then given in terms of the pressure $P(X,Y)$ by

$$\mathbf{U} = (U,V) = -\frac{K}{\mu}\nabla P, \quad \nabla = (\partial_X, \partial_Y). \tag{1}$$

Incompressibility of the feed solution requires

$$\nabla\cdot\mathbf{U} = 0 \quad\Rightarrow\quad \nabla\cdot(K\nabla P) = 0, \tag{2}$$

within the support layers. We assume flow is driven by an imposed pressure difference, P_0. We further assume a no-flux condition at pleat tips and valleys. Boundary conditions are as follows:

$$P^+(0,Y) = P_0, \quad P^+_X(L,Y) = 0, \quad P^+_Y(X,H) = 0, \quad P^-_X(0,Y) = 0, \quad P^-(L,Y) = 0, \quad P^-_Y(X,-H) = 0, \tag{3}$$

where we use $\pm$ superscripts to distinguish between quantities evaluated in $Y \gtrless 0$ respectively. Assuming unidirectional flow (Y-direction) within the membrane, the Darcy law for the flow velocity $V_{\rm m}$ through the membrane then gives

$$|V_{\rm m}| = \frac{K_{\rm m}}{\mu D}\left[P^+\big|_{Y=D/2} - P^-\big|_{Y=-D/2}\right], \qquad 0 \le X \le L, \tag{4}$$

where, by continuity of flux, $|V_{\rm m}(X)| = |V(X,D/2)| = |V(X,-D/2)|$ (with V as defined in (1)). $K_{\rm m}$ will vary in both time and space due to fouling: $K_{\rm m}(X,T)$. The local pore radius $A(X,Y,T)$ (see figure 2) changes in time due to the adsorptive fouling, modeled by accounting for particle transport and deposition within pores. Following earlier work (Sanaei & Cummings, 2017), we propose a simple advection model for the particle concentration $C(X,Y,T)$ within pores,

$$V_{\rm p}\frac{\partial C}{\partial Y} = -\Lambda\frac{C}{A}, \quad C(X,\frac{D}{2},T) = C_0. \tag{5}$$

The constant Λ measures the strength of attraction between the particles and the pore wall that gives rise to the deposition. The pore radius shrinks in response to the deposition: consistent with (5) we propose

$$\frac{\partial A(X,Y,T)}{\partial T} = -\Lambda\alpha C(X,Y,T), \quad A(X,Y,0) = A_0(Y), \tag{6}$$

for some constant α (proportional to the particle size). This formulation with $A_0(Y)$ assumes that all pores in the membrane are identical initially. We will later briefly consider initial pore profiles that can vary in X also, to investigate the possible effect of nonuniform pore size distribution in the plane of the membrane.

2.2 Asymptotic Analysis and Model Summary

We introduce dimensionless variables and parameters via the following scalings

$$(X,Y,Y,P^\pm,C,A) = (Lx, Hy, D\tilde{y}, P_0p^\pm, C_0c, Wa), \quad \epsilon = H/L, \quad \delta = D/H,$$

where $\epsilon \ll 1$, $\delta \ll 1$, and then seek asymptotic solutions as follows:

$$p^+(x,y) = p_0^+(x,y) + \epsilon^2 p_1^+(x,y) + \cdots, \quad p^-(x,y) = p_0^-(x,y) + \epsilon^2 p_1^-(x,y) + \cdots$$

We obtain the following asymptotic model equations, valid to leading order in ϵ and δ:

$$p_{0xx}^+(x,t) = \frac{\Gamma(p_0^+(x,t) - p_0^-(x,t))}{r_{\rm m}(x,t)}, \quad p_0^+(0,t) = 1, \quad p_{0x}^+(1,t) = 0, \tag{7}$$

$$-p_{0xx}^-(x,t) = \frac{\Gamma(p_0^+(x,t) - p_0^-(x,t))}{r_{\rm m}(x,t)}, \quad p_0^-(1,t) = 0, \quad p_{0x}^-(0,t) = 0, \tag{8}$$

$$\frac{\partial c(x,\tilde{y},t)}{\partial \tilde{y}} = \frac{\lambda a(x,\tilde{y},t)c(x,\tilde{y},t)r_{\rm m}(x,t)}{p_0^+(x) - p_0^-(x)}, \quad c(x,\frac{1}{2},t) = 1, \tag{9}$$

$$\frac{\partial a(x,\tilde{y},t)}{\partial t} = -c(x,\tilde{y},t), \quad a(x,\tilde{y},0) = a_0(\tilde{y}), \tag{10}$$

where $r_{\rm m}(x,t) = \int_{-\frac{1}{2}}^{\frac{1}{2}} \frac{d\tilde{y}}{a^4(x,\tilde{y},t)}$, represents the dimensionless membrane resistance at location x and time t, and $\Gamma = \frac{K_{\rm m0}}{K\epsilon^2\delta}$, and $\lambda = \frac{\pi\mu D^2\Lambda}{4WK_{\rm m0}P_0}$ are model parameters.

3. Results

3.1 Definitions for Filter Performance Evaluation and Optimization

To evaluate filter performance and to carry out design optimization, we first define some key quantities:

$$\text{flux}(t) = \int_0^1 |v_{\rm m}(x,t)|dx\,, \tag{11}$$

$$\text{throughput}(t) = \int_0^t \text{flux}(\tau)d\tau\,. \tag{12}$$

The plot of flux versus throughput is a standard characterization of membrane performance in the filtration literature, and is therefore a tool that we also use here. The instantaneous x-averaged particle concentration $c_{\rm avg}(t)$ at the downstream side of the membrane $\tilde{y} = -1/2$, another important physical quantity when considering the particle removal capability of the membrane, is defined as:

$$c_{\rm avg}(t) = \frac{\int_0^1 v_{\rm m}(x,t)c(x,-\frac{1}{2},t)dx}{\text{flux}(t)}. \tag{13}$$

We also monitor the accumulated particle concentration of the filtrate, $c_{\rm acm}(t)$, defined as:

$$c_{\rm acm}(t) = \frac{\int_0^t\int_0^1 v_{\rm m}(x,\tau)c(x,-\frac{1}{2},\tau)dxd\tau}{\text{throughput}(t)}, \tag{14}$$

(if all the filtrate is collected in a jar as the filtration progresses, then $c_{\rm acm}(t)$ is the particle concentration of the collected filtrate in the jar at time t). We consider the optimization process as finding the pore profile that gives *highest total throughput* while maintaining the *initial particle removal threshold* (denoted by R) *above a certain percentage* at time $t = 0$ ($c_{\rm avg}(0) \le 1 - R$). In our example simulations that follow, the particle removal threshold is set at $R = 99\%$, or $R = 99.9\%$. The cost function we minimize based on this optimization case is defined as:

$$\text{Cost function} = \begin{cases} -(\text{total throughput}) & \text{if no constraint is violated,} \\ 1 & \text{if physical constraint is violated,} \\ 2 & \text{if threshold constraint is violated.} \end{cases} \tag{15}$$

We optimize for the initial pore profile $a_0(\tilde{y})$ within the class of low-order polynomials (linear, quadratic, cubic).

3.2 Effect of λ on Optimization

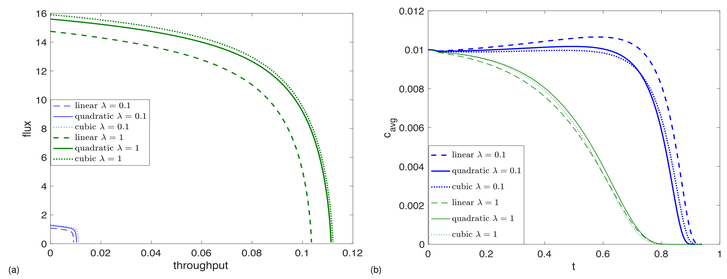

Figure 3: *Results with particle removal threshold $R = 99\%$, $\lambda = 1$ (green) and $\lambda = 0.1$ (blue), for optimal pore profiles from classes of linear, quadratic and cubic polynomials: (a) Flux-throughput plots for all cases; (b) Instantaneous averaged particle concentration $c_{\rm avg}(t)$ in filtrate for optimized profiles.*

For $R = 99\%$, "stickier" wall (indicated by greater λ) gives higher total throughput. Particle retention may deteriorate over time (Fig. 3(b)).

3.3 Effect of R on Optimization

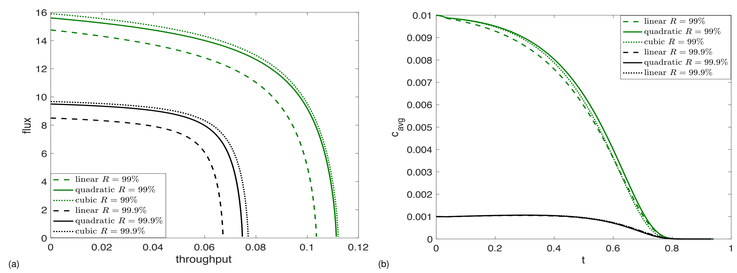

Figure 4: *Results for membranes with optimized pore profiles from the classes of linear, quadratic and cubic polynomials, with $\lambda = 1$ and $R = 99\%$ (green) or $R = 99.9\%$ (black): (a) Flux-throughput plots; (b) Instantaneous averaged particle concentration $c_{\rm avg}(t)$ in the filtrate.*

If we insist on removing more particles ($R = 99.9\%$) we reduce the instantaneous flux and the total throughput.

3.4 Optimization with in-plane (X-direction) Pore-size Variation

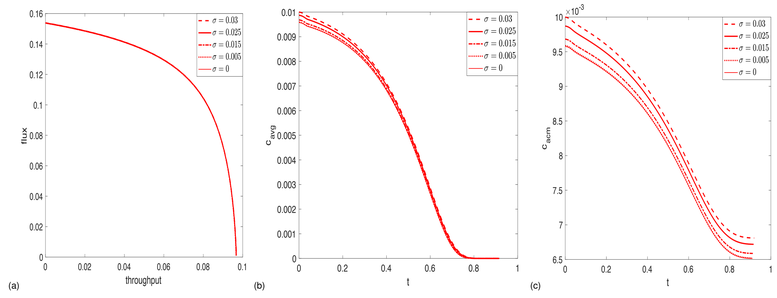

Figure 5: *Effect of in-plane pore-size variations of the form $a(x,\tilde{y},0) = \mathrm{A}(\tilde{y})(1+\sigma\sin(2n\pi x))$. (a-c) show results based on this initial pore profile, optimized with $\sigma = 0.03$, $n = 10$ and $\mathrm{A}(\tilde{y})$ linear, for $\lambda = 1$, $R = 99\%$. (a) Flux-throughput plots, (b) $c_{\rm avg}(t)$ plots, (c) $c_{\rm acm}(t)$ plots, for $\sigma = 0, 0.005, 0.015, 0.025, 0.03$.*

Figures 5(a-c) collectively indicate that if the manufacture has a reliable upper bound on the in-plane pore-size variation, they could aim to manufacture membranes with the optimized initial pore profile based on this bound. As long as the bound holds, the resulting profile will yield almost the optimized total throughput, without violating the particle removal requirement.

4. Conclusions

- We have formulated a general membrane optimization problem based on maximizing throughput subject to a particle removal constraint.
- Within a given function class (polynomials) we are able to find the optimized pore profile in terms of polynomials. The optimized profiles converge as the degree of polynomial increases.
- Our model reveals that particle retention may worsen over time (as observed experimentally).
- We have proposed a possible approach for optimization accounting for manufacturing variations.
- Future work will account for multiple particle species and more general optimization.

5. Acknowledgements

The authors acknowledge financial support from the NSF under grant DMS-1615719.

References

Sun, Y. X., Sanaei, P., Kondic, L., Cummings, L. J. Modeling and design optimization for pleated membrane filters (in preparation).

Sanaei, P., Richardson, G.W., Witelski, T., Cummings, L.J. Flow and fouling in a pleated membrane filter. *J. Fluid Mech.* **795**, 36-59 (2016).

Sanaei, P., Cummings, L.J. Flow and fouling in membrane filters: effects of membrane morphology. *J. Fluid Mech.* **818**, 744-771 (2017).